

9. FRICTION LOSS ALONG A PIPE

Introduction

In hydraulic engineering practice, it is frequently necessary to estimate the head loss incurred by a fluid as it flows along a pipeline. For example, it may be desired to predict the rate of flow along a proposed pipe connecting two reservoirs at different levels. Or it may be necessary to calculate what additional head would be required to double the rate of flow along an existing pipeline.

Loss of head is incurred by fluid mixing which occurs at fittings such as bends or valves, and by frictional resistance at the pipe wall. Where there are numerous fittings and the pipe is short, the major part of the head loss will be due to the local mixing near the fittings. For a long pipeline, on the other hand, skin friction at the pipe wall will predominate. In the experiment described below, we investigate the frictional resistance to flow along a long straight pipe with smooth walls.

Friction Loss in Laminar and Turbulent Pipe Flow

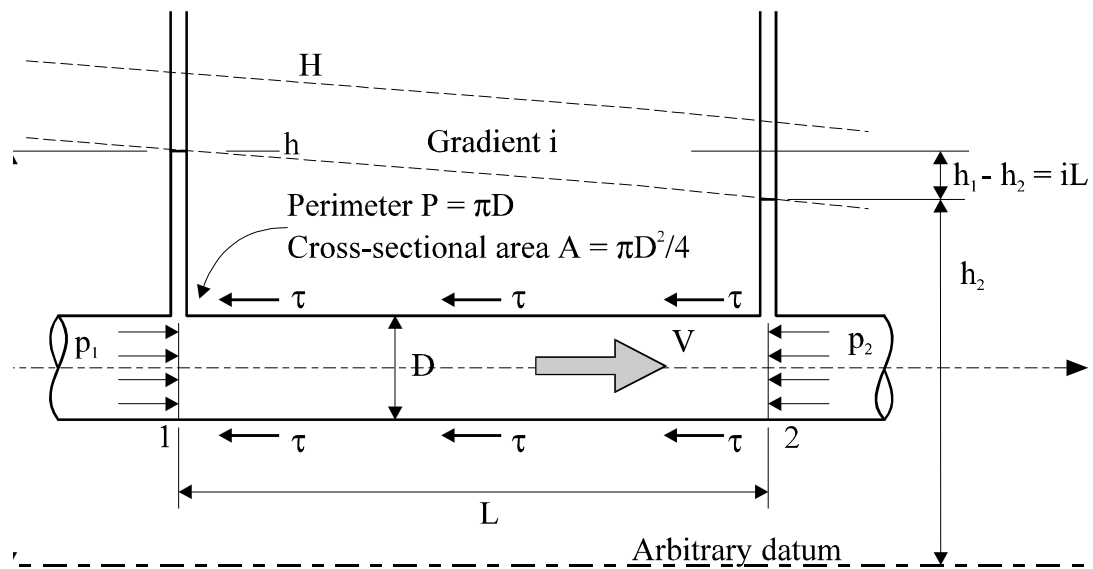


Fig 9.1 Illustration of fully developed flow along a pipe

Fig 9.1 illustrates flow along a length of straight uniform pipe of diameter D . All fittings such as valves or bends are sufficiently remote as to ensure that any disturbances due to them have died away, so that the distribution of velocity across the

pipe cross section does not change along the length of pipe under consideration. Such a flow is said to be "fully developed". The shear stress τ at the wall, which is uniform around the perimeter and along the length, produces resistance to the flow. The piezometric head h therefore falls at a uniform rate along the length, as shown by the piezometers in Fig 9.1. Since the velocity head is constant along the length of the pipe, the total head H also falls at the same rate.

The slope of the piezometric head line is frequently called the "hydraulic gradient", and is denoted by the symbol i :

$$i = \frac{-dh}{dl} = \frac{-dH}{dl} \quad (9.1)$$

(The minus signs are due to the fact that head decreases in the direction of increasing l , which is measured positive in the same sense as the velocity V . The resulting value of i is then positive). Over the length L between sections 1 and 2, the fall in piezometric head is

$$h_1 - h_2 = iL \quad (9.2)$$

Expressed in terms of piezometric pressures p_1 and p_2 at sections 1 and 2:

$$p_1 - p_2 = w_iL = \rho g i L \quad (9.3)$$

in which w is the specific weight and ρ the density of the water.

There is a simple relationship between wall shear stress τ and hydraulic gradient i . The pressures p_1 and p_2 acting on the two ends of the length L of pipe produce a net force. This force, in the direction of flow, is

$$(p_1 - p_2)A$$

in which A is the cross-sectional area of the pipe. This is opposed by an equal and opposite force, generated by the shear stress τ acting uniformly over the surface of the pipe wall. The area of pipe wall is PL , where P is the perimeter of the cross section, so the force due to shear stress is

$$\tau \cdot PL$$

Equating these forces:

$$(p_1 - p_2)A = \tau.PL$$

This reduces, by use of Equation (9.3), to

$$\tau = \left(\frac{A}{P}\right)\rho g i^\dagger \quad (9.4)$$

Now expressing A and P in terms of pipe diameter D, namely, $A = \pi D^2/4$ and $P = \pi D$ so that $(A/P) = D/4$, we obtain the result:

$$\tau = \left(\frac{D}{4}\right)\rho g i \quad (9.5)$$

We may reasonably expect that τ would increase in some way with increasing rate of flow. The relationship is not a simple one, and to understand it we must learn something about the nature of the motion, first described by Osborne Reynolds in 1883. By observing the behaviour of a filament of dye introduced into the flow along a glass tube, he demonstrated the existence of two different types of motion. At low velocities, the filament appeared as a straight line passing down the whole length of the tube, indicating smooth or laminar flow. As the velocity was gradually increased in small steps, he observed that the filament, after passing a little way along the tube, mixed suddenly with the surrounding water, indicating a change to turbulent motion. Similarly, if the velocity were decreased in small steps, a transition from turbulent to laminar motion suddenly occurred. Experiments with pipes of different diameters and with water at various temperatures led Reynolds to conclude that the parameter which determines whether the flow shall be laminar or turbulent in any particular case is

$$Re = \frac{\rho V D}{\mu} = \frac{V D}{\nu} \quad (9.6)$$

in which

$Re =$ **Reynolds number** of the motion

$\rho =$ Density of the fluid

[†]The term (A/P) which appears here is frequently called the "hydraulic radius" or "hydraulic mean depth", and may be applied to cross sections of any shape.

- $V = Q/A$ denotes the mean velocity of flow, obtained by dividing the discharge rate Q by the cross sectional area A
- $\mu =$ Coefficient of absolute viscosity of the fluid
- $\nu = \mu/\rho$ denotes the coefficient of kinematic viscosity of the fluid

Note that the Reynolds number is dimensionless, as may readily be checked from the following:

$$\rho [M L^{-3}] \quad \mu [M L^{-1} T^{-1}] \quad \nu [L^2 T^{-1}] \quad V [L T^{-1}] \quad D [L]$$

The motion will be laminar or turbulent according as to whether the value of Re is less than or greater than a certain critical value. Experiments made with increasing flow rates show that the critical value of Re for transition to turbulent flow depends on the degree of care taken to eliminate disturbances in the supply and along the pipe. On the other hand, experiments with decreasing flow rates show that transition to laminar flow takes place at a value of Re which is much less sensitive to initial disturbance. This lower value of Re is found experimentally to be about 2000. Below this, the pipe flow becomes laminar sufficiently downstream of any disturbance, no matter how severe.

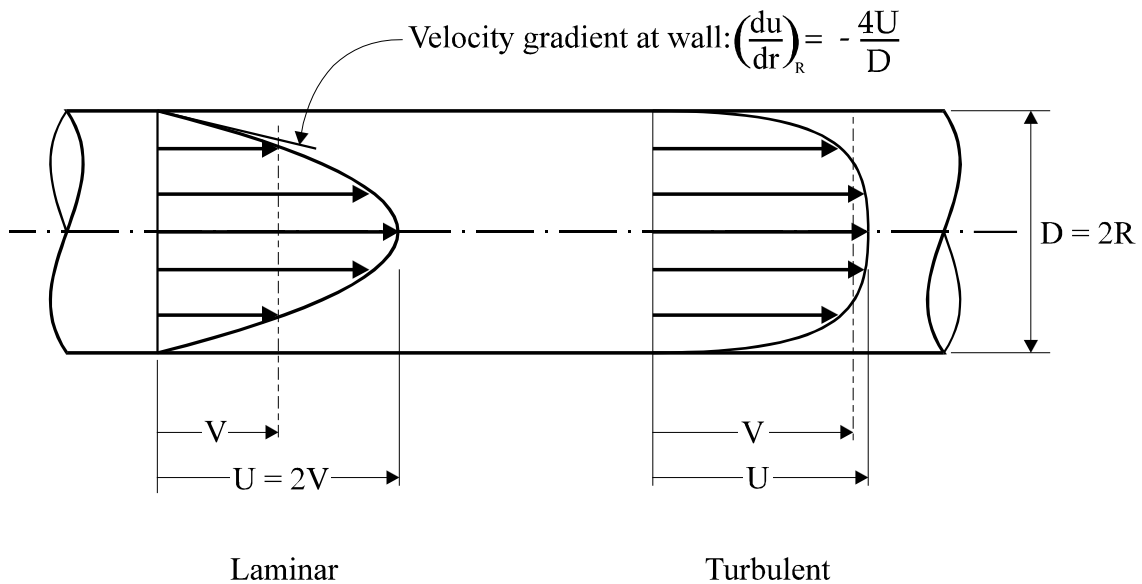


Fig 9.2 Velocity distributions in laminar and turbulent pipe flows

Fig 9.2 illustrates the difference between velocity profiles across the pipe cross sections in laminar and in turbulent flow. In each case the velocity rises from zero at

the wall to a maximum value U at the centre of the pipe. The mean velocity V is of course less than U in both cases.

In the case of laminar flow, the velocity profile is parabolic[‡]. The ratio U/V of centre line velocity to mean velocity is

$$\frac{U}{V} = 2 \quad (9.7)$$

and the velocity gradient at the wall is given by

$$\left(\frac{du}{dr}\right)_R = \frac{-4U}{D} = \frac{-8V}{D} \quad (9.8)$$

so that the wall shear stress τ due to fluid viscosity is

$$\tau = \frac{8\mu V}{D} \quad (9.9)$$

Substituting for τ in Equation (9.5) from this equation leads to the result

$$i = \frac{32\nu V}{gD^2} \quad (9.10)$$

which is one form of Poiseuille's equation.

In the case of turbulent flow, the velocity distribution is much flatter over most of the pipe cross section. As the Reynolds number increases, the profile becomes increasingly flat, the ratio of maximum to mean velocity reducing slightly. Typically, U/V falls from about 1.24 to about 1.12 as Re increases from 10^4 to 10^7 .

Because of the turbulent nature of the flow, it is not possible now to find a simple expression for the wall shear stress, so the value has to be found experimentally. When considering such experimental results, we might reasonably relate the wall

[‡]The derivation of the parabolic velocity profile, and of the Poiseuille equation, is given in many standard textbooks.

shear stress τ to the mean velocity pressure ρV^2 . So a dimensionless **friction factor f** could be defined by

$$\tau = f \cdot \rho V^2 \quad (9.11)$$

The hydraulic gradient i may now be expressed in terms of f by use of Equation (9.5), and the following result is readily obtained:

$$i = \frac{4f V^2}{D 2g} \quad (9.12)$$

Therefore, the head loss ($h_1 - h_2$) between sections 1 and 2 of a pipe of diameter D , along which the mean flow velocity is V , is seen from Equation (9.2) to be given by

$$h_1 - h_2 = 4f \frac{L V^2}{D 2g} \quad (9.13)$$

where L is the length of pipe run between the sections. This is frequently referred to as Darcy's equation.

The results of many experiments on turbulent flow along pipes with smooth walls have shown f to be a slowly decreasing function of Re . Various correlations of the experimental data have been proposed, one of which is

$$\frac{1}{\sqrt{f}} = 4 \log(Re \sqrt{f}) - 0.4 \quad (9.14)$$

This expression, which is due to Prandtl, fits experimental results well in the range of Re from 10^4 to 10^7 , although it does have the slight disadvantage that f is not given explicitly.

Another correlation, due to Blasius, is:

$$f = 0.079 Re^{-1/4} \quad (9.15)$$

This gives explicit values which are in agreement with those from the more complicated Equation (9.14) to within about 2% over the limited range of Re from 10^4 to 10^5 . Above 10^5 , however, the Blasius equation diverges substantially from experiment.

We have seen that when the flow is turbulent it is necessary to resort to experiment to find f as a function of Re. However, in the case of laminar flow, the value of f may be found theoretically from Poiseuille's equation. Equating the expressions for i in Equations (9.10) and (9.12):

$$\frac{32 \nu V}{g D^2} = \frac{4f V^2}{D 2g}$$

After reduction this gives the result

$$f = \frac{16}{\text{Re}} \tag{9.16}$$

In summary, the hydraulic gradient i may conveniently be expressed in terms of a dimensionless wall friction factor f . This factor has the theoretical value $f = 16/\text{Re}$ for laminar flow along a smooth walled pipe. There is no corresponding theoretical for turbulent flow, but good correlation of many experimental results on smooth walled pipes is given by equations such as (9.14) and (9.15).

Description of Apparatus

The apparatus is illustrated in Fig 9.3. Water from a supply tank is led through a flexible hose to the bell-mouthed entrance of a straight tube along which the friction loss is measured. Piezometer tapings are made at an upstream section which lies approximately 45 tube diameters away from the pipe entrance, and approximately 40 diameters away from the pipe exit. These clear lengths upstream and downstream of the test section are required to ensure that the results are not affected by disturbances originating at the entrance or the exit of the pipe. The piezometer tapings are connected to an inverted U-tube manometer, which reads head loss directly in mm of water gauge, or to a U-tube containing water and mercury to cover higher values of head loss.

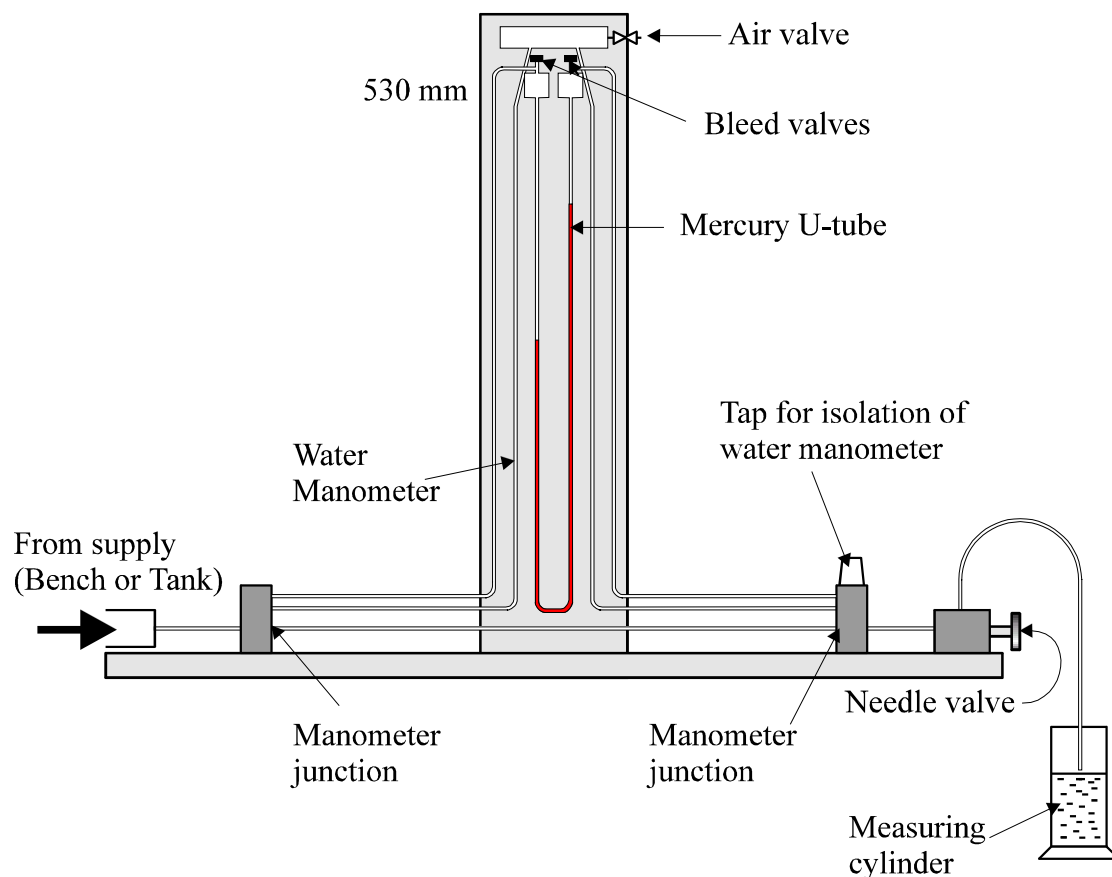


Fig 9.3 Apparatus for measuring friction loss along a pipe

The rate of flow along the pipe is controlled by a needle valve at the pipe exit, and may be measured by timing the collection of water in a beaker which is weighed on a laboratory scale or measured in a volumetric cylinder. (The discharge rate is so small as to make the use of the bench measuring tank quite impractical).

Experimental Procedure

The apparatus is set on the bench and levelled so that the manometers stand vertically. The water manometer is then connected to the piezometer by opening the tap at the downstream piezometer connection. The bench supply valve is then carefully opened and adjusted until there is a steady flow down the overflow pipe from the supply tank, so that it provides a constant head to the pipe under test. With the needle valve partly open to allow water to flow through the system, any trapped air is removed by manipulation of the flexible connecting pipes. Particular care should be taken to clear all air from the piezometer connections. The needle valve is then closed, whereupon

the levels in the two limbs of the manometer should settle to the same value. If they do not, check that the flow has been stopped absolutely, and that all air has been cleared from the piezometer connections. The height of the water level in the manometer may be raised to a suitable level by allowing air to escape through the air valve at the top, or may be depressed by pumping in air through the valve.

The first reading of head loss and flow may now be taken. The needle valve is opened fully to obtain a differential head of at least 400 mm, and the rate of flow measured. If a suitable laboratory scale, weighing to an accuracy of 1 g, is available, the discharge is collected over a timed interval and then weighed. If a volumetric cylinder is used, the time required to collect a chosen volume is measured. During the period of collection, ensure that the outlet end of the flexible tube is below the level of the bench, and that it never becomes immersed in the discharged water. Otherwise, the differential head and rate of flow may change, especially at the lower flow rates. It is recommended that the manometer is read several times during the collection period, and a mean value of differential head taken. The needle valve is then closed in stages, to provide readings at a series of reducing flow rates. The water temperature should be observed as accurately as possible at frequent intervals.

These readings should comfortably cover the whole of the laminar flow region and the transition from turbulent flow. It is advisable to plot a graph of differential head loss against flow rate as the experiment proceeds to ensure that sufficient readings have been taken to establish the slope of the straight line in the region of laminar flow.

To obtain a range of results with turbulent flow it is necessary to use water from the bench supply and to measure differential heads with the mercury-water U-tube. The supply hose from the overhead tank is disconnected and replaced by one from the bench supply pipe. Since the equipment will be subjected to the full pump pressure, the joints should be secured using hose clips. The water manometer is isolated by closing the tap at the downstream piezometer connection. With the pump running, the bench supply valve is opened fully, and the needle valve opened slightly, so that there is a moderate discharge from the pipe exit. The bleed valves at the top of the U-tube are then opened to flush out any air in the connecting tubes. Manipulation of the tubes will help to fill the whole length of the connections from the piezometer tapplings right up to the surfaces of the mercury columns in the U-tube. The bleed valves and needle valve are then closed, and a check is made that the U-tube shows no differential reading. If it does not, further attempts should be made to clear the connections of air. Readings of head loss and flow rate are now taken, starting at the maximum available

discharge rate, and reducing in stages, using the needle valve to set the desired flow rates. The water temperature should be recorded at frequent intervals. It is desirable to provide some overlap of the ranges covered by the mercury U-tube and the water manometer. Noting that 1 mm differential reading on the mercury-water U-tube represents 12.6 mm differential water gauge, a few readings should be taken below about 40 mm on the mercury-water U-tube.

The diameter D of the tube under test, and the length L between the piezometer tapings, should be noted.

Results and Calculations

Length of pipe between piezometer tapings $L = 524 \text{ mm}$

Diameter of pipe $D = 3.00 \text{ mm}$

Cross sectional area of pipe $\pi D^2/4$ $A = 7.069 \text{ mm}^2 = 7.069 \times 10^{-6} \text{ m}^2$

Qty (ml)	t (s)	h₁ (mm)	h₂ (mm)	θ (°C)	V (m/s)	i	log i	10³f	log f	Re	log Re
400	50.8	521.0	56.0	15.3	1.114	0.887	-0.052	10.52	-1.978	2954	3.471
400	54.0	500.0	85.0		1.048	0.792	-0.101	10.61	-1.974	2779	3.444
400	58.8	476.0	114.0		0.962	0.691	-0.161	10.98	-1.960	2552	3.407
400	61.8	452.0	145.0		0.916	0.586	-0.232	10.28	-1.988	2428	3.385
400	67.2	427.5	174.0		0.842	0.484	-0.315	10.04	-1.998	2233	3.349
300	57.8	390.0	223.0	15.3	0.734	0.319	-0.497	8.70	-2.061	1947	3.290
300	71.9	375.0	245.0		0.590	0.248	-0.605	10.48	-1.980	1565	3.195
300	93.9	362.0	263.0		0.457	0.189	-0.724	13.32	-1.875	1211	3.083
200	92.4	349.0	282.0		0.306	0.128	-0.893	20.07	-1.698	812	2.910
150	100.8	340.0	295.5		0.211	0.085	-1.071	28.20	-1.550	558	2.747
85	113.6	332.5	306.0	15.3	0.106	0.051	-1.296	66.41	-1.178	280	2.448
50	129.5	325.0	316.0		0.055	0.017	-1.765	84.71	-1.072	144	2.161

Table 9.1 Results with water manometer §

§ A great amount of repetitive computation is required to reduce the results shown in Tables 9.1 and 9.2. Students are encouraged to use a programmable pocket calculator or to write a suitable program for use on a computer for reducing the experimental data.

Qty (ml)	t (s)	h ₁ (mm)	h ₂ (mm)	θ (°C)	V (m/s)	i	log i	10 ³ f	log f	Re	log Re
900	39.0	431.0	195.0	15.5	3.265	5.675	0.754	7.83	-2.106	8704	3.940
900	42.9	414.0	214.0		2.968	4.809	0.682	8.03	-2.095	7913	3.898
900	46.6	402.0	226.0		2.732	4.232	0.627	8.34	-2.079	7285	3.862
900	51.7	390.0	240.0	15.5	2.463	3.607	0.557	8.75	-2.058	6566	3.817
900	58.0	377.0	254.5		2.195	2.946	0.469	8.99	-2.046	5853	3.767
900	62.7	370.5	261.0		2.031	2.633	0.420	9.40	-2.027	5414	3.734
900	68.5	362.0	270.5		1.859	2.200	0.342	9.37	-2.028	5006	3.700
600	47.5	358.5	275.0		1.787	2.008	0.303	9.25	-2.034	4813	3.682
600	54.6	351.5	283.5	15.9	1.555	1.635	0.214	9.96	-2.002	4187	3.622
600	70.4	340.0	294.0		1.206	1.106	0.044	11.20	-1.955	3248	3.512
300	48.0	331.5	305.5		0.884	0.625	-0.204	11.77	-1.929	2382	3.377

Table 9.2 Results with mercury manometer

θ°C	0	1	2	3	4	5	6	7	8	9
10	1.307	1.271	1.236	1.202	1.170	1.140	1.110	1.082	1.055	1.029
20	1.004	0.980	0.957	0.935	0.914	0.893	0.873	0.854	0.836	0.818
30	0.801	0.784	0.769	0.753	0.738	0.724	0.710	0.696	0.683	0.658

Table 9.3 Table of $10^6 v$ (m^2/s) as a function of water temperature $\theta^\circ C$

Tables 9.1 and 9.2 present typical results obtained using the water and mercury manometers, and Table 9.3 gives values of $10^6 v$, expressed in units of m^2/s , as a function of water temperature $\theta^\circ C$, in the range from $10^\circ C$ to $39^\circ C$.

Values of v , which are needed to compute Reynolds numbers, may be obtained by interpolation from this table. Alternatively, they may be obtained from the empirical formula

$$10^6 v = 1.0049 - 0.02476(\theta - 20) + 0.00044(\theta - 20)^2 \quad (9.17)$$

which fits experimentally measured values of v very well over the range of θ from $15^\circ C$ to $30^\circ C$.

In Table 9.1, values of i are obtained simply from

$$i = \frac{(h_1 - h_2)}{L}$$

For example, in the first line of the table,

$$i = \frac{(521.0 - 56.0)}{524} = 0.887$$

and $\log i$, used for graphical representation, is

$$\log i = \log 0.887 = -0.052$$

To obtain the friction factor f , we first compute the velocity head as follows:

In the first line of the table, for example, the flow rate Q is

$$Q = \frac{Qty}{t} = \frac{400 \times 10^{-6}}{50.8} = 7.874 \times 10^{-6} \text{ m}^3/\text{s}$$

so the velocity V along the pipe is

$$V = \frac{Q}{A} = \frac{7.874 \times 10^{-6}}{7.069 \times 10^{-6}} = 1.114 \text{ m/s}$$

The velocity head is then

$$\frac{V^2}{2g} = \frac{1.114^2}{(2 \times 9.81)} = 0.0632 \text{ m}$$

Equation (9.12) may now be used to find f :

$$i = \frac{4f V^2}{D 2g}$$

so that

$$f = i \frac{D}{4} \frac{1}{V^2/2g}$$

and inserting numerical values for the first line of the table,

$$f = 0.887 \times \frac{3.00 \times 10^{-3}}{4} \times \frac{1}{0.0632} = 10.52 \times 10^{-3}$$

Then

$$\log f = \log(10.52 \times 10^{-3}) = -1.978$$

Finally, Reynolds number Re is obtained from the definition

$$\text{Re} = \frac{VD}{\nu}$$

in which ν is found by interpolation from Table 9.3, or from Equation (9.17), to have the value

$$\nu = 1.131 \times 10^{-6} \text{ m}^2/\text{s}$$

at the relevant temperature of 15.3°C.

Hence

$$\text{Re} = \frac{1.114 \times 3.00 \times 10^{-3}}{1.131 \times 10^{-6}} = 2954$$

and

$$\log \text{Re} = 3.471$$

Calculations for Table 9.2, containing results using the mercury-water manometer, are done in identical fashion, except that the differential heads recorded from the manometer need to be expressed as equivalent heads of water by multiplication by the factor 12.6. So the hydraulic gradient now becomes

$$i = \frac{12.6(h_1 - h_2)}{L}$$

In the first line of Table 9.2, for example,

$$i = \frac{12.6(431.0 - 195.0)}{524} = 5.675$$

Fig 9.4 Diagram of mercury-water U-tube

Fig 9.4 shows how the factor 12.6 arises. The pressure applied to the left hand limb of the mercury-water U-tube is greater than that applied at the right, so the mercury is driven down to point U in the right hand limb and up to point T in the right. The difference of levels of these points is $(h_1 - h_2)$. Now the pressures p_u and p_v at points U and V shown on the diagram are equal, since these points are at the same level, and are connected hydrostatically round the bottom of the U-tube. The difference of pressure between U and S in the left hand limb, due to a water column of height $(h_1 - h_2)$ and specific weight w , is

$$p_u - p_s = w(h_1 - h_2)$$

In the right hand limb, the mercury column of height $(h_1 - h_2)$ has specific weight sw , where s is the specific gravity of mercury, so the pressure difference between V and T is

$$p_v - p_t = sw(h_1 - h_2)$$

Subtracting these results, and recalling that $p_u = p_v$, we obtain

$$p_s - p_t = (s - 1) w(h_1 - h_2)$$

Expressing this as a differential head of water of specific weight w , we see that

$$h_s - h_t = (s - 1)(h_1 - h_2)$$

The specific gravity s of mercury is 13.6, so that

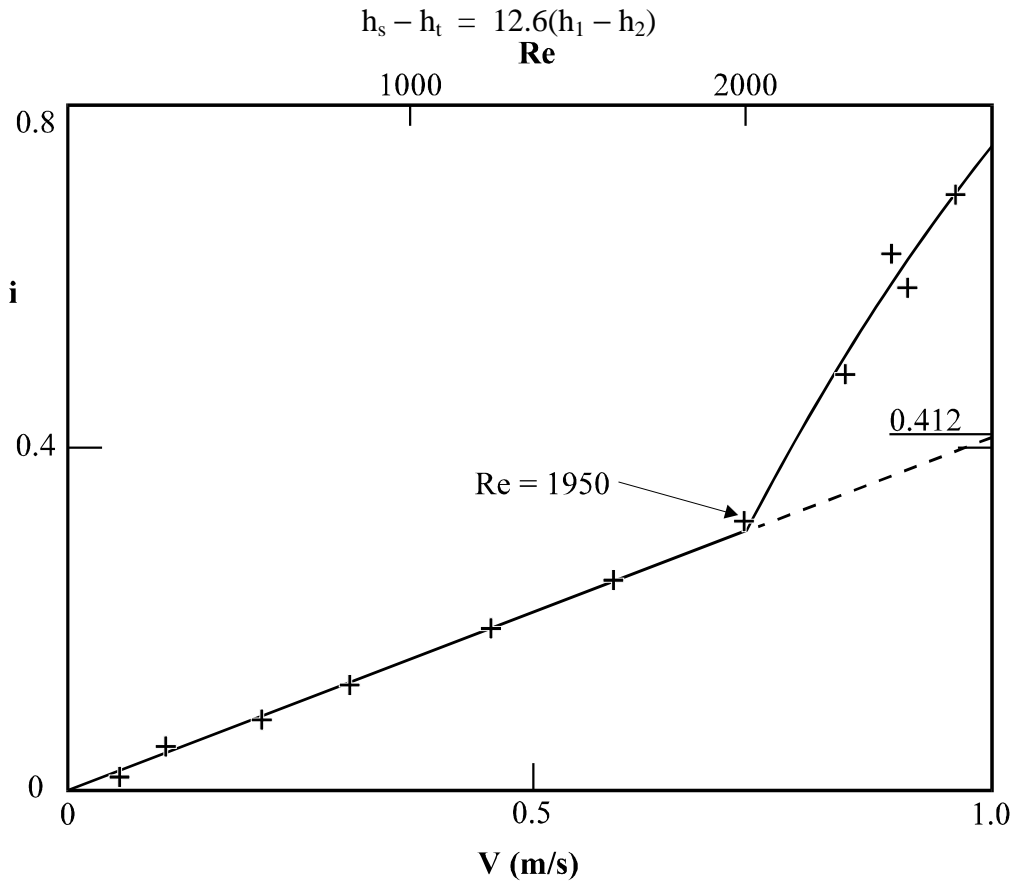


Fig 9.5 Variation of hydraulic gradient i with velocity V up to 1 m/s

Fig 9.5 shows how the hydraulic gradient varies in proportion to flow velocity V over a range from zero to the critical value, above which the proportionality does not apply. The critical value of Re for transition from turbulent to laminar flow (the experiment having been performed with decreasing flow rate) is 1950. Equation (9.10), which is a form of Poiseuille's equation, may be used to infer the coefficient of kinematic viscosity from measurements in the region of laminar flow. From the graph, the slope of the linear portion is found to be

$$\frac{i}{V} = 0.412 \text{ s/m}$$

Rewriting Equation (9.10) in the form

$$v = \frac{g}{32 V} D^2$$

and inserting numerical values,

$$v = \frac{9.81}{32} \times 0.412 \times (3.00 \times 10^{-3})^2$$

$$v = 1.137 \times 10^{-6} \text{ m}^2/\text{s}$$

Within the limits of experimental error, this agrees with the value $v = 1.131 \times 10^{-6} \text{ m}^2/\text{s}$ obtained from the standard data of Table 9.3 at the working temperature of 15.3°C , so confirming the validity of Poiseuille's equation in the laminar flow regime.

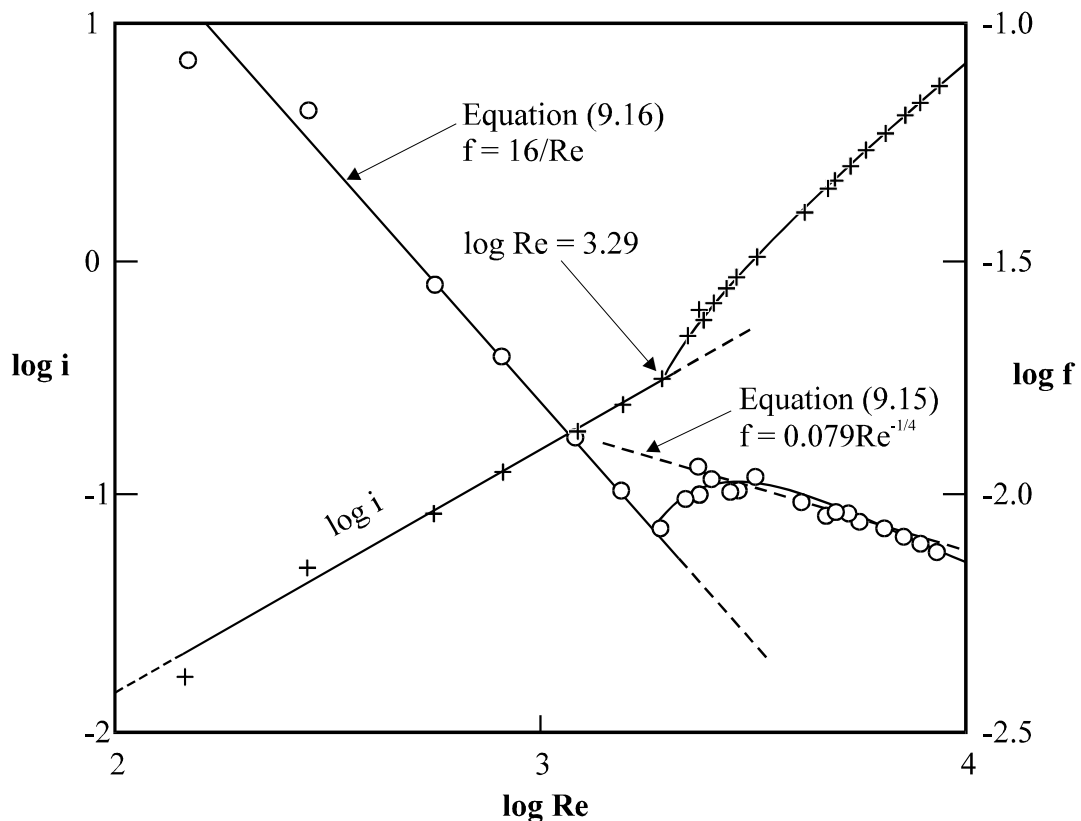


Fig 9.6 Variation of $\log i$ with $\log Re$

Fig 9.6 shows logarithmic graphs of both hydraulic gradient i and friction factor f as functions of Reynolds number Re . Transition occurs at the value $\log Re = 3.29$, viz $Re = 1950$. The straight line corresponding to Equation (9.16) for laminar flow is shown on the figure, and it is clear that excellent agreement with experiment is obtained. This follows, of course, from the good correspondence which has been found between the value of v obtained from Poiseuille's equation and the value obtained from standard data. The straight line corresponding to the Blasius Equation (9.15) for turbulent flow is also shown. In the range of $\log Re$ from 3.29 to 3.43 (Re

from 1950 to 2710), f rises along a curve as Re increases. For higher values of Re , a fair agreement with the Blasius friction factor is found.

Questions for Further Discussion

1. What suggestions do you have for improving the apparatus?
2. What percentage changes in the computed values of V , i , f , v and Re would you expect to result from,
 - i) An error of 1.0 mm in measurement of L ;
 - ii) An error of 0.03 mm in measurement of D .
3. A possible project is the adaptation of the apparatus to operation with air instead of water. Using values of μ and ν taken from physical tables, calculate the likely critical velocity and the corresponding pressure drop. Consider whether this could be measured using a water U-tube. Devise a simple method of producing a steady flow of air at a known rate by displacement from a closed vessel.

10. LOSSES AT PIPE FITTINGS

Introduction

As described in Chapter 9, loss of head along a pipeline is incurred both by frictional resistance at the wall along the run of the pipe, and at fittings such as bends or valves. For long pipes with few fittings, the overall loss is dominated by wall friction. If, however, the pipe is short and there are numerous fittings, then the principal losses are those which are produced by disturbances caused by the fittings. In the experiment described below, we investigate losses at various fittings, typical of those which are used frequently in pipe systems.

Measurement of Loss of Total Head at a Fitting

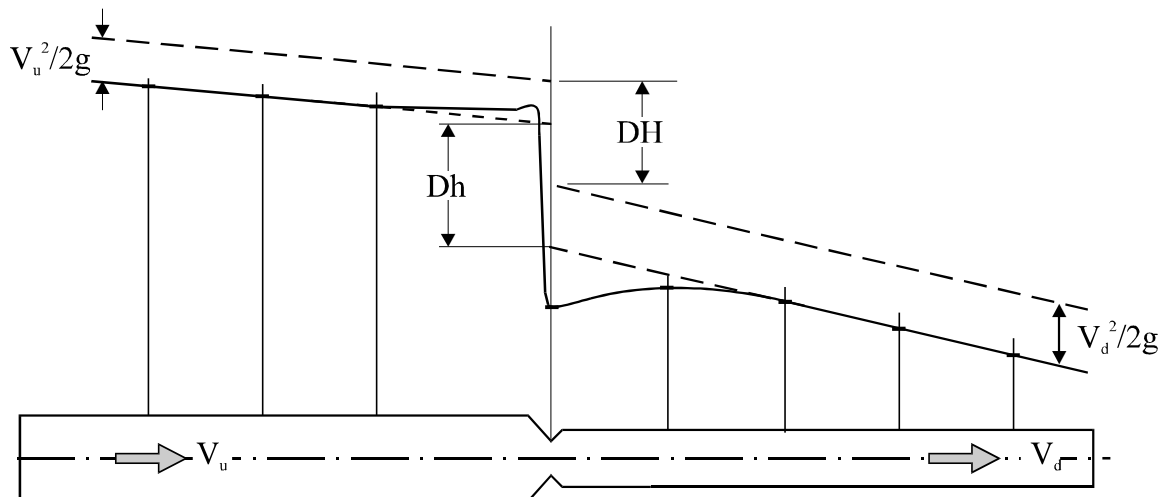


Fig 10.1 Schematic representation of loss at a pipe fitting

Fig 10.1 shows water flowing at speed V_u along a pipe of diameter D_u towards some pipe fitting such as a bend or a valve, but shown for simplicity as a simple restriction in the cross section of the flow. Downstream of the fitting, the water flows along a pipe of some other diameter D_d , along which the velocity of flow is V_d . The figure indicates the variation of piezometric head along the pipe run, as would be shown by numerous pressure tappings at the pipe wall. In the region of undisturbed flow, far upstream of the fitting, the distribution of velocity across the pipe remains unchanged from one cross section to another; this is the condition of **fully developed pipe flow** which is considered in Chapter 9. Over this region, the piezometric head falls with a

uniform, mild gradient, as a result of constant friction at the pipe wall in the fully developed flow. Close to the fitting, however, there are sharp and substantial local disturbances to the piezometric head, caused by rapid changes in direction and speed as the water passes through the fitting. In the downstream region, these disturbances die away, and the line of piezometric head returns asymptotically to a slight linear gradient, as the velocity distribution gradually returns to the condition of fully developed pipe flow.

If the upstream and downstream lines of linear friction gradient are now extrapolated to the plane of the fitting, a loss of piezometric head Δh due to the fitting is found. To establish the corresponding loss of total head ΔH it is necessary to introduce the velocity heads in the upstream and downstream runs of pipe. From Fig 10.1 it is clear that

$$\Delta H = \Delta h + \frac{V_u^2}{2g} - \frac{V_d^2}{2g} \quad (10.1)$$

It is convenient to express this in terms of a dimensionless **loss coefficient** K , by dividing through by the velocity head in either the upstream or the downstream pipe (the choice depending on the context, as we shall see later). The result is

$$K = \frac{\Delta H}{V_u^2/2g} \quad \text{or} \quad \frac{\Delta H}{V_d^2/2g} \quad (10.2a)$$

For the case where $D_u = D_d$, the flow velocities in the upstream and downstream pipes are identical, so we may simplify the definition to

$$K = \frac{\Delta H}{V^2/2g} \quad \text{or} \quad \frac{\Delta h}{V^2/2g} \quad (10.2b)$$

where V denotes the flow velocity in either the upstream or the downstream pipe run[†]. To obtain results of high accuracy, long sections of straight pipe, (of 60 pipe diameters or more), are needed to establish with certainty the relative positions of the linear

[†] The velocity head $V^2/2g$ used here is based simply on the mean flow velocity V . Because the velocity varies across the pipe cross section, from zero at the wall to a maximum at the centre, the velocity head also varies over the cross section. The mean value of velocity head in this non-uniform flow is somewhat higher, being typically 1.05 to 1.07 $V^2/2g$ when the flow is turbulent.

sections of the piezometric lines. Such long upstream and downstream lengths are impracticable in a compact apparatus such as the one described below. Instead, just two piezometers are used, one placed upstream and the other downstream of the fitting, at sufficient distances as to avoid severe disturbances. These show the piezometric head loss $\Delta h'$ **between the tappings**. An estimate is then made of the friction head loss Δh_f which would be incurred in fully developed flow along the run of pipe between the piezometer tappings. The piezometric head difference Δh **across the fitting** is then found by subtraction:

$$\Delta h = \Delta h' - \Delta h_f \quad (10.3)$$

Characteristics of Flow through Bends and at Changes in Diameter

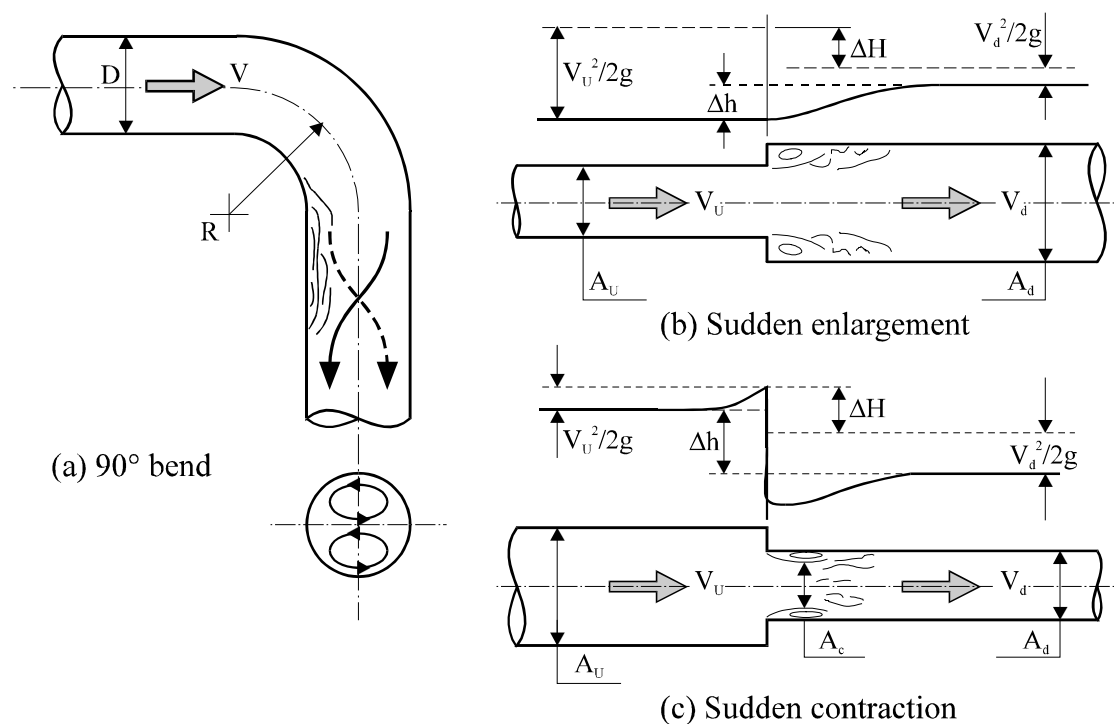


Fig 10.2 Flow in a bend, sudden enlargement and sudden contraction

Fig 10.2(a) illustrates flow round a 90° bend which has a constant circular cross section of diameter D . The radius of the bend is R , measured to the centre line. The curvature of the flow as it passes round the bend is caused by a radial gradient of piezometric head, so that the piezometric head is lower at the inner surface of the pipe than at its outer surface. As the flow leaves the bend, these heads start to equalise as

the flow loses its curvature, so that the piezometric head begins to rise along the inner surface. This rise causes the flow to separate, so generating mixing losses in the subsequent turbulent reattachment process. Additionally, the radial gradient of piezometric head sets up a secondary cross-flow in the form of a pair of vortices, having outward directed velocity components near the pipe centre, and inward components near the pipe walls. When superimposed on the general streaming flow, the result is a double spiral motion, which persists for a considerable distance in the downstream flow, and which generates further losses that are attributable to the bend. Clearly, the value of the loss coefficient K will be a function of the geometric ratio R/D ; as this ratio increases, making the bend less sharp, we would expect the value of K to fall. The smallest possible value of R/D is 0.5, for which the bend has a sharp inner corner. For this case, the value of K is usually about 1.4. As R/D increases, the value of K falls, reducing to values which may be as low as 0.2 as R/D increases up to 2 or 3. There is also a slight dependence on Reynolds number Re .

Fig 10.2(b) shows the flow in a sudden enlargement. The flow separates at the exit from the smaller pipe, forming a jet which diffuses into the larger bore, and which reattaches to the wall some distance downstream. The vigorous turbulent mixing, resulting from the separation and reattachment of the flow, causes a **loss of total head**. The **piezometric head** in the emerging jet, however, starts at the same value as in the pipe immediately upstream, and **increases through the mixing region**, so rising across the enlargement. These changes in total and piezometric head, neglecting the effect of friction gradient, are illustrated in the figure. Assuming that the piezometric pressure on the face of the enlargement to be equal to that in the emerging jet, and that the momentum flux is conserved, the loss of total head may be shown to be

$$\Delta H = \frac{(V_u - V_d)^2}{2g} \quad (10.4)$$

The corresponding **rise** in piezometric head is

$$\Delta h = \frac{2V_d(V_u - V_d)}{2g} \quad (10.5)$$

The loss coefficient K is in this case best related to the upstream velocity V_u so that

$$K = \frac{(V_u - V_d)^2/2g}{V_u^2/2g} = \left[1 - \frac{V_d}{V_u}\right]^2 = \left[1 - \frac{A_u}{A_d}\right]^2 \quad (10.6)$$

This indicates that K increases from zero when $A_u/A_d = 1.0$ (the case when there is no enlargement), to 1.0 when A_u/A_d falls to zero.

Consider lastly the sudden contraction shown in Fig 10.2(c). The flow separates from the edge where the face of the contraction leads into the smaller pipe, forming a jet which converges to a contracted section of cross sectional area A_c . Beyond this contracted section there is a region of turbulent mixing, in which the jet diffuses and reattaches to the wall of the downstream pipe. The losses occur almost entirely in the process of turbulent diffusion and reattachment. The losses are therefore expected to be those due to an enlargement from the contracted area A_c to the downstream pipe area A_d . Following the result of Equation (10.4), the expected loss of total head in contraction is

$$\Delta H = \frac{(V_c - V_d)^2}{2g} \quad (10.7)$$

The obvious choice of reference velocity in this case is V_d , so the loss coefficient K becomes

$$K = \left[\frac{V_d}{V_c} - 1\right]^2 = \left[\frac{A_d}{A_c} - 1\right]^2 \quad (10.8)$$

Consider now the probable range of values of A_d/A_c . If the value of the pipe contraction ratio is 1.0, that is if $A_d/A_u = 1.0$, then there is in effect no contraction and there will be no separation of the flow, so $A_d/A_c = 1.0$. Equation (10.8) then gives a zero value of K . If, however, the contraction is very severe, viz. $A_d/A_u \rightarrow 0$, then the upstream pipe tends to an infinite reservoir in comparison with the downstream one. We might then reasonably expect the flow at the entry to the downstream pipe to resemble that from a large reservoir through an orifice of area A_d . For such an orifice, the contraction coefficient has the value 0.6 approximately, so that

$$\frac{A_d}{A_c} = \frac{1}{0.6} = 1.667$$

Substituting this value in Equation (10.7) gives

$$K = 0.44$$

It might therefore be expected that K would rise from zero when the pipe area ratio $A_d/A_u = 1$ to a value of about 0.44 as the ratio A_d/A_u falls towards zero.

Description of Apparatus

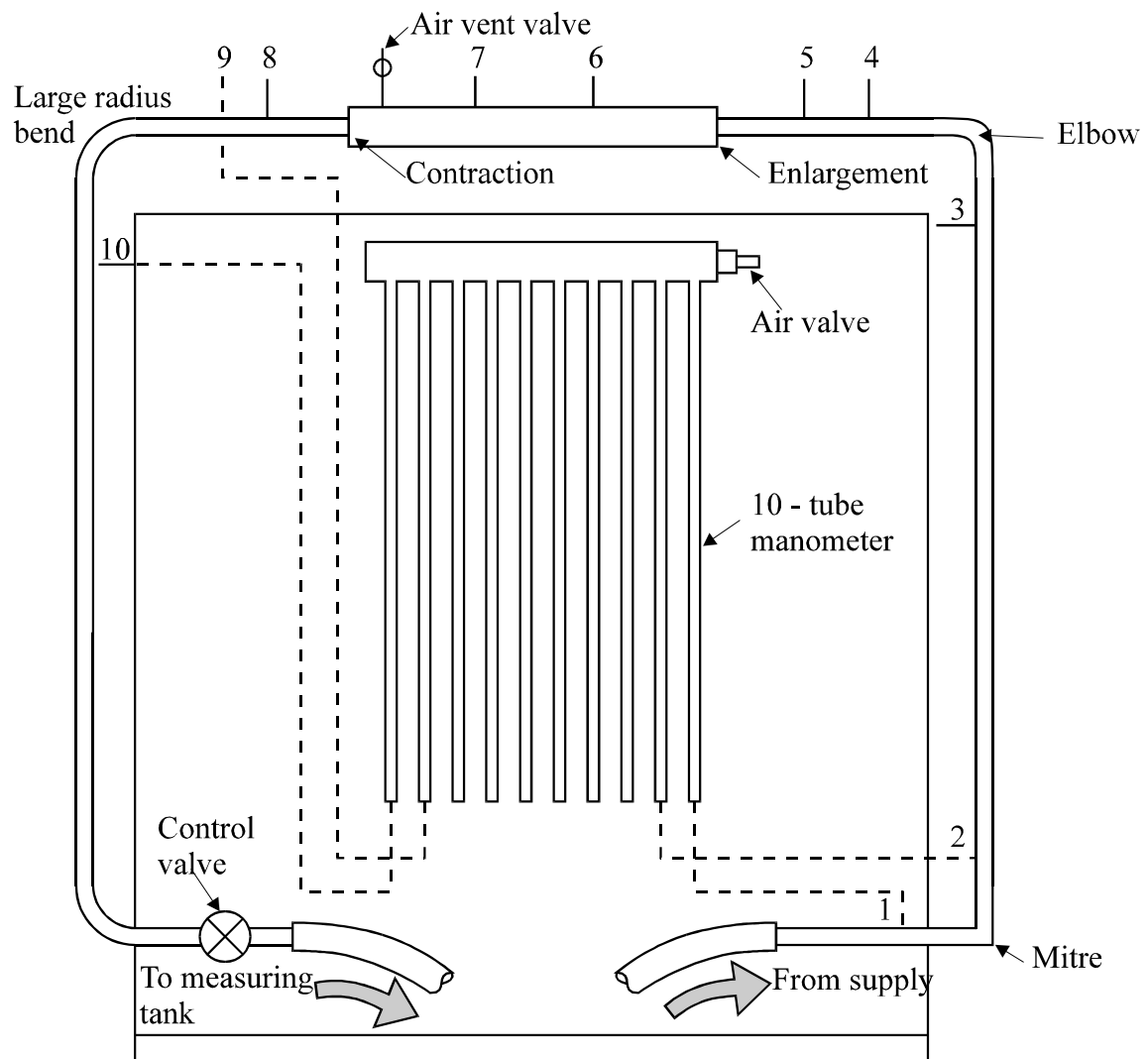


Fig 10.3 Arrangement of apparatus for measuring losses in pipe fittings

Several arrangements of apparatus are available, incorporating selections of fittings in various configurations. The particular equipment illustrated in Fig 10.3 has the

advantage of portability. It may be operated from the H1 Hydraulic Bench. It provides a run of pipework, made up of components manufactured in rigid plastic material, supported in the vertical plane from a baseboard with a vertical panel at the rear. Water is supplied to the pipe inlet from the hydraulic bench, and is discharged at the exit to the measuring tank. In the run of the pipe there are the following fittings:

- 90° mitre bend
- 90° elbow bend
- 90° large radius bend
- Sudden enlargement in pipe diameter
- Sudden contraction in pipe diameter

Piezometer tappings are provided in the pipe wall, at clear lengths of 4 pipe diameters, upstream and downstream of each of the fittings. The tappings are connected to a glass multitube manometer which may be pressurised using a bicycle pump. The system may be purged of air by venting to atmosphere through the manometer, and through a vent valve at the highest point of the pipe run. The flow rate through the equipment may be varied by adjusting the valve near the pipe exit.

Experimental Procedure

Details of procedure will vary according to the facilities provided by the particular equipment in use. The following description applies to the equipment illustrated in Fig 10.3.

The diameters of the pipes and dimensions of the fittings, as shown on the mimic diagram, are noted. The supply hose of the Hydraulic Bench is connected to the pipework inlet. A further hose is fixed to the exit pipe, so that the discharge from the equipment flows into the measuring tank of the bench. The pump is then started, and the control valve at the exit is opened to allow water to circulate through the pipework.

To ensure that all air is expelled from the system, the air valve at the top of the manometer is slackened or removed completely, and the vent valve at the top of the pipework is opened. The control valve at the exit is then partially closed, so that the pressure inside the pipework drives water out through the vent at the top of the pipework and through the piezometers, along the connecting tubes, and up the

manometer tubes. This flow of water will carry air bubbles along with it. The control valve should be closed sufficiently as to produce vigorous flow out of the air vent valve and the manometer, so ensuring that the system is thoroughly purged of air. When this is complete, the air vent valve should be closed, and the manometer air valve replaced and tightened. The cycle pump is then used to drive the water levels in the manometer tubes down to a convenient set of heights.

With the exit valve closed, the levelling screws are then used to set the scale of the manometer board perfectly horizontal, i.e. to show a uniform reading across the board.

The apparatus is now ready for use. The exit valve is opened carefully, while the water levels are observed in the manometer tubes. Air is admitted or released as necessary to keep all the readings within the range of the scale. When the maximum feasible flow rate is reached, differential piezometer readings across each of the fittings are recorded, while the collection of a known quantity of water in the measuring tank of the bench is timed. These measurements are repeated at a number of rates of flow. It may be necessary to pump in more air to the manometer to keep the readings within bounds as the exit valve is closed; alternatively the bench valve may be used to effect part of the flow reduction. If it is thought that air might have collected at the top of the pipework, this may at any time be checked by opening the air vent for a short time.

Results and Calculations

Dimensions of Pipes and Fittings

Diameter of smaller bore pipe	$D_1 = 22.5 \text{ mm}$	$A_1 = 3.98 \times 10^{-4} \text{ m}^2$
Diameter of larger bore pipe	$D_2 = 29.6 \text{ mm}$	$A_2 = 6.88 \times 10^{-4} \text{ m}^2$
Radius to centre line of elbow	$R_e = 35.0 \text{ mm}$	
Radius to centre line of bend	$R_b = 69.1 \text{ mm}$	
Length of straight pipe between piezometer tapping and fitting	$4D_1$ or $4D_2$	

If the measured flow rate is Q l/s, then the velocities V_1 and V_2 along the pipes of cross sectional A_1 and A_2 m^2 areas are:

$$V_1 = 10^{-3} Q/A_1 \text{ m/s and } V_2 = 10^{-3} Q/A_2 \text{ m/s}$$

or

$$V_1 = 2.515 Q \text{ m/s and } V_2 = 1.453 Q \text{ m/s}$$

Differential Piezometer Readings and Loss of Total Head

			Differential Piezometer Head $\Delta h'$ (mm)				
Qty (1)	Time (s)	Q (l/s)	Mitre 1-2	Elbow 3-4	Enlrg't 5-6	Cont'n 7-8	Bend 9-10
24	43.3	0.554	154	113	-28	109	62
24	45.8	0.524	148	102	-26	100	58
24	46.7	0.514	126	93	-25	89	55
12	26.0	0.462	104	77	-19	71	45
12	28.1	0.427	90	64	-12	63	39
12	30.6	0.392	75	58	-14	52	28
12	36.5	0.329	53	40	-10	36	22

Table 10.1 Piezometric head losses at various rates of flow

Table 10.1 gives a typical set of results as recorded in the laboratory. Differential piezometric heads $\Delta h'$ between piezometer tapplings are tabulated in sequence in the direction of flow, viz. tapplings 1 and 2 are upstream and downstream of the mitre bend, 3 and 4 upstream and downstream of the elbow, and so on. Note that the reading for the enlargement is negative, showing an **increase of piezometric head at the enlargement**.

					Loss of Total Head ΔH (mm)				
Q (kg/s)	V_1 (m/s)	V_2 (m/s)	$V_1^2/2g$ (mm)	$V_2^2/2g$ (mm)	Mitre 1-2	Elbow 3-4	Enlrg't 5-6	Cont'n 7-8	Bend 9-10
0.554	1.394	0.806	99.0	33.0	135	88	25	30	31
0.524	1.318	0.762	88.5	29.5	131	79	21	29	30
0.514	1.293	0.747	85.2	28.4	109	71	20	21	28
0.462	1.161	0.671	68.8	23.0	91	59	18	16	24
0.427	1.074	0.621	58.8	19.6	78	49	19	16	21
0.392	0.986	0.570	49.5	16.5	65	45	12	12	12
0.329	0.827	0.478	34.9	11.6	46	31	9	8	11

Table 10.2 Total head losses at various rates of flow

Table 10.2 shows the head losses ΔH across each of the fittings, as computed from the measurements of $\Delta h'$ in Table 10.1. The computations first use an estimate of the head loss Δh_f , due to friction between piezometer tapings, to find the piezometric head loss Δh from Equation (10.3). If the velocity downstream of the fitting is the same as that upstream, Equation (10.3) shows that the total head loss ΔH is the same as the piezometric head loss Δh . This is the case for the mitre, elbow and bend. If, however, there is a change in velocity from upstream to downstream, then Equation (10.3) is used to compute total head loss ΔH from the piezometric head loss Δh .

The friction head loss is estimated by choosing a suitable value of friction factor f for fully developed flow along a smooth pipe. Several options are available, and the choice used here is the Prandtl equation quoted in Chapter 9:

$$\frac{1}{\sqrt{f}} = 4 \log(\text{Re}\sqrt{f}) - 0.4 \quad (9.14)$$

Typical values derived from this equation, are presented in Table 10.3.

10^{-4} Re	1.0	1.5	2.0	2.5	3.0	3.5
$10^3 f$	7.73	6.96	6.48	6.14	5.88	5.67

Table 10.3 Friction factor f for smooth walled pipe

It would be possible to evaluate friction factors for each individual flow rate. However, since f varies only slowly with Re , and the friction loss is generally fairly small in relation to the measured value of $\Delta h'$, it suffices to establish the value of f at just one typical flow rate, at about the middle of the range of measurement.

Choosing the typical flow rate $Q = 0.45$ l/s, which is close to the mid range of Table 10.1, and assuming the value $\nu = 1.00 \times 10^{-6}$ m²/s for the coefficient of kinematic viscosity, then for the smaller bore pipe:

$$D_1 = 22.5 \text{ mm and } V_1 = 2.515 \times 0.45 = 1.132 \text{ m/s}$$

so

$$\text{Re}_1 = V_1 \frac{D_1}{\nu} = \frac{1.132 \times 22.5 \times 10^{-3}}{1.00 \times 10^{-6}} = 2.55 \times 10^4$$

Similarly for the larger bore pipe:

$$D_2 = 29.6 \text{ mm and } V_2 = 1.453 \times 0.45 = 0.654 \text{ m/s}$$

so

$$Re_2 = V_2 \frac{D_2}{\nu} = \frac{0.654 \times 29.6 \times 10^{-3}}{1.00 \times 10^{-6}} = 1.94 \times 10^4$$

The values of friction factor at these two Reynolds numbers may be found from Table 10.3 by interpolation to be

$$f_1 = 0.00611 \text{ and } f_2 = 0.00654$$

These are the values to be used to correct the observed differential heads $\Delta h'$ in Table 10.1. For example, consider the mitre bend. The pipe diameter is D_1 , and the distance between the piezometers, measured along the pipe centreline, is given by

$$\frac{L_1}{D_1} = 8$$

Now Darcy's equation, presented as Equation (9.13) in Chapter 9, gives the frictional head loss Δh_f as

$$\Delta h_f = 4f_1 \left(\frac{L_1}{D_1} \right) \frac{V_1^2}{2g}$$

Inserting numerical values:

$$\Delta h_f = 4 \times 0.0061 \times 8 \frac{V_1^2}{2g} = 0.196 \frac{V_1^2}{2g}$$

In the first line of Table 10.2, therefore:

$$\Delta h_f = 0.196 \frac{V_1^2}{2g} = 0.196 \times 99 = 19.4, \text{ say } 19 \text{ mm}$$

The piezometric head loss Δh across the mitre is then, according to Equation (10.3),

$$\Delta h = \Delta h' - \Delta h_f = 154 - 19 = 135 \text{ mm}$$

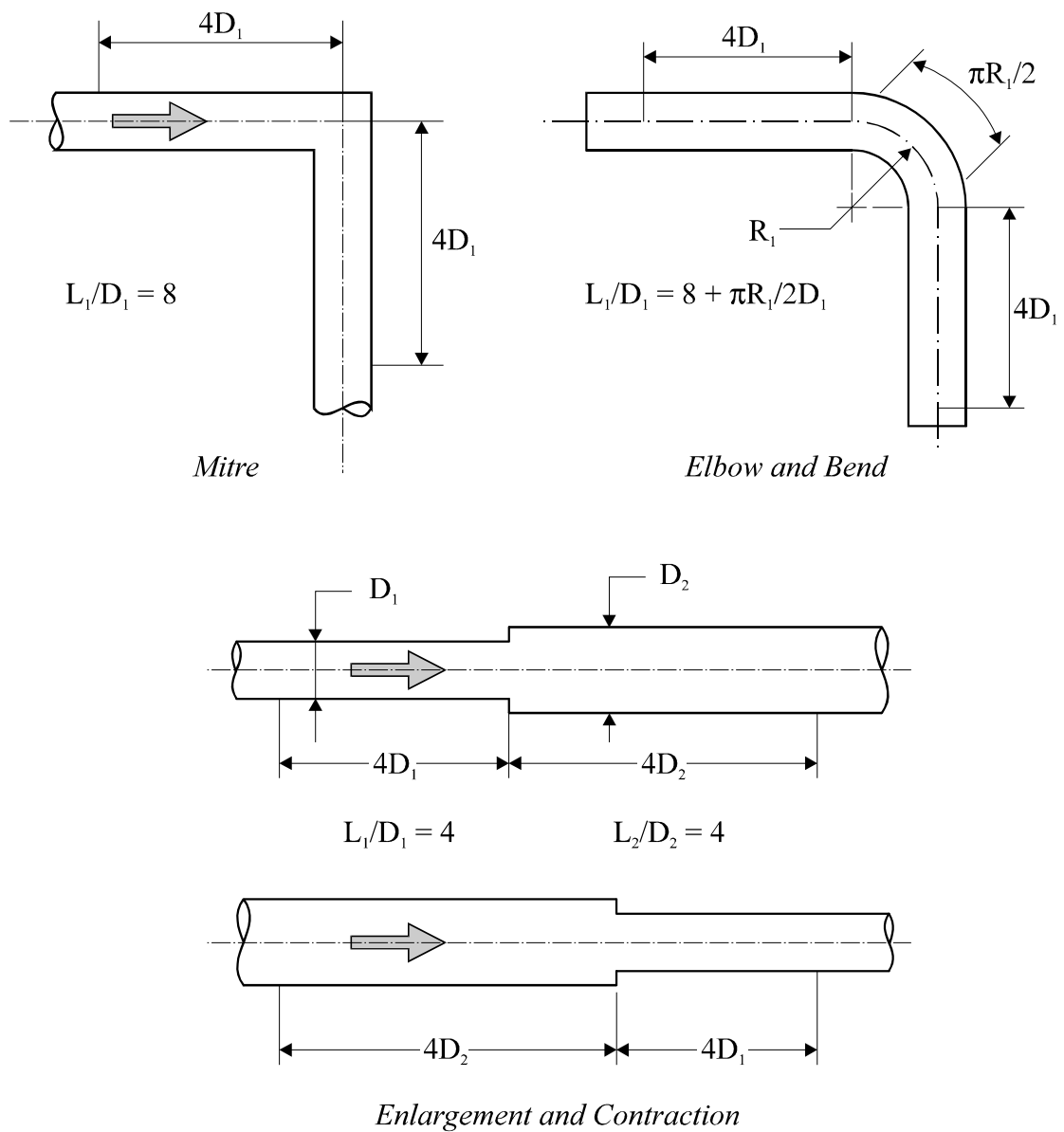


Fig 10.4 Illustration of positions of piezometer tappings

Since there is no change in velocity from upstream to downstream of the mitre, this is also the loss of total head ΔH , and the figure 135 is therefore entered in the first line of Table 10.2.

Similar calculations are made for the elbow and bend, using the relationship shown in Fig 10.4:

$$\frac{L_1}{D_1} = 8 + \frac{\pi R_1}{2D_1}$$

This leads to

$$\Delta h_f = 0.257 \frac{V_1^2}{2g} \text{ for the elbow}$$

and

$$\Delta h_f = 0.313 \frac{V_1^2}{2g} \text{ for the bend.}$$

In the first line of results, for example,

$$\Delta h_f = 0.257 \times 99.0 = 25.4 \text{ mm so } \Delta H = 113 - 25.4 = 87.6, \text{ say } 88 \text{ mm for the elbow}$$

$$\Delta h_f = 0.313 \times 99.0 = 31.0 \text{ mm so } \Delta H = 62 - 31.0 = 31.0, \text{ say } 31 \text{ mm for the bend}$$

In the case of the enlargement, the sum of friction losses in the pipes of diameter D_1 upstream and of diameter D_2 downstream is

$$\Delta h_f = 4f_1 \left(\frac{L_1}{D_1} \right) \frac{V_1^2}{2g} + 4f_2 \left(\frac{L_2}{D_2} \right) \frac{V_2^2}{2g}$$

Noting dimensions from Fig 10.4 and inserting numerical values:

$$\Delta h_f = 4 \times 0.00611 \times 4 \frac{V_1^2}{2g} + 4 \times 0.00654 \times 4 \frac{V_2^2}{2g}$$

or

$$\Delta h_f = 0.098 \frac{V_1^2}{2g} + 0.105 \frac{V_2^2}{2g}$$

In the first line of Table 10.2, then, for the enlargement:

$$\Delta h_f = 0.098 \times 99.0 + 0.105 \times 33.0 = 13.2 \text{ mm}$$

The change in piezometric head is then, from Equation (10.3),

$$\Delta h = \Delta h' - \Delta h_f = -28 - 13.2 = -41.2 \text{ mm}$$

To derive the change ΔH in total head, Equation (10.1) is used:

$$\Delta H = \Delta h + \frac{V_1^2}{2g} + \frac{V_2^2}{2g} = -41.2 + 99.0 - 33.0 = 24.8, \text{ say } 25 \text{ mm}$$

This is the value entered in the first line of Table 10.2. Similarly for the contraction, where Δh_f has the same value as for the enlargement. The computation is:

$$\Delta h = \Delta h' - \Delta h_f = 109 - 13.2 = -95.8 \text{ mm}$$

$$\Delta H = \Delta h + \frac{V_2^2}{2g} - \frac{V_1^2}{2g} = 95.8 + 33.0 - 99.0 = 29.8, \text{ say } 30 \text{ mm}$$

which is also shown on the first line of Table 10.2.

Derivation of Loss Coefficients K

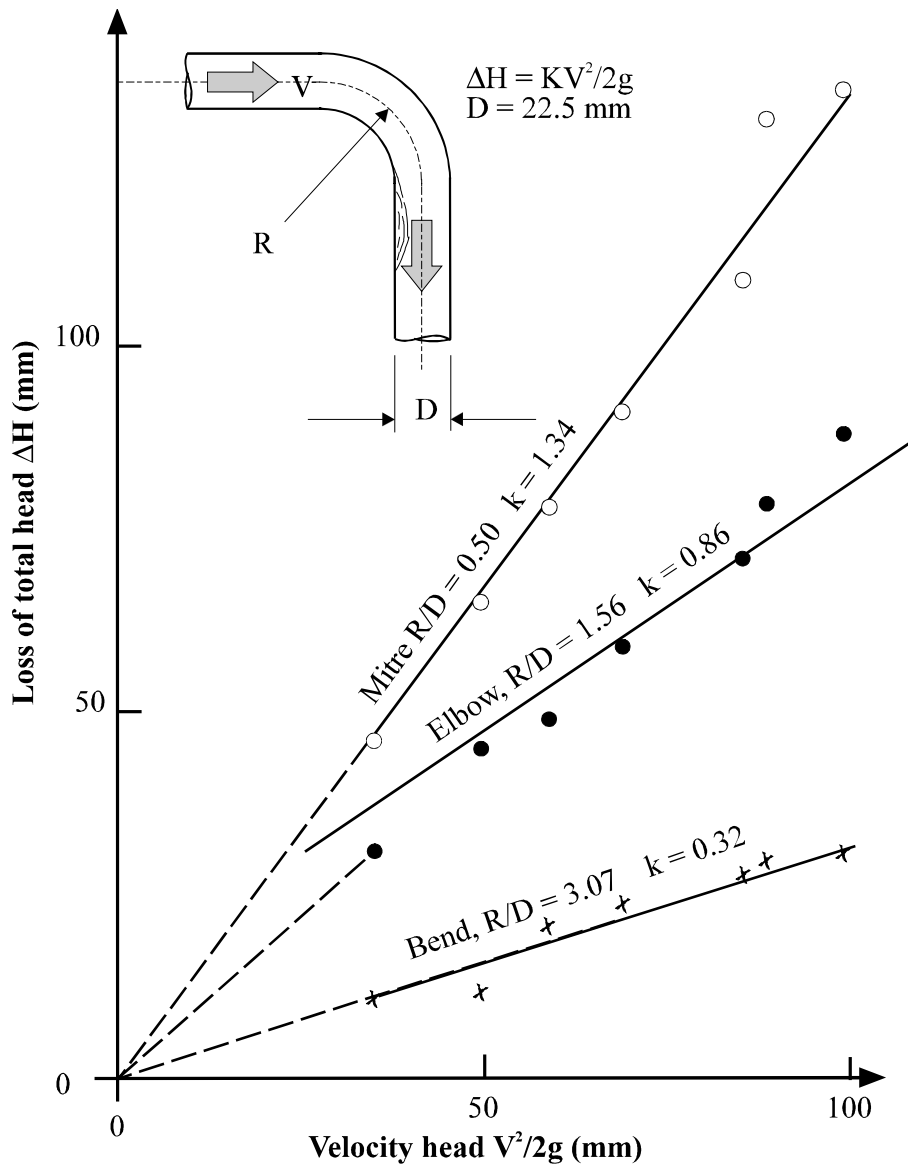
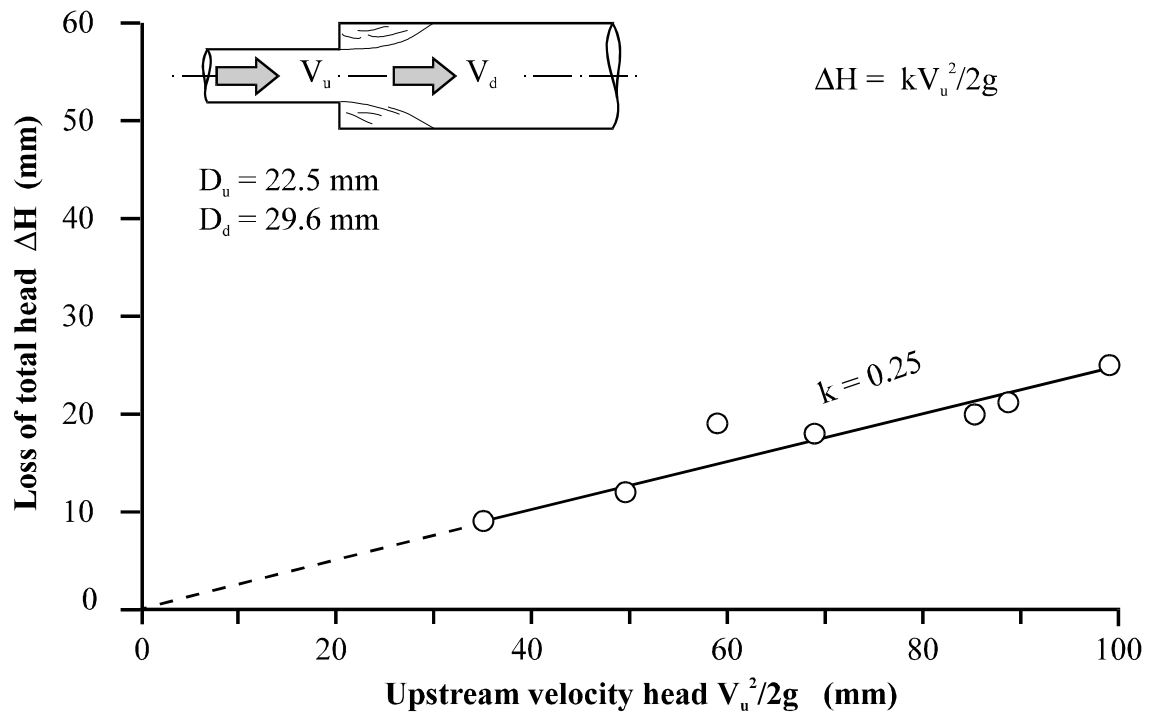
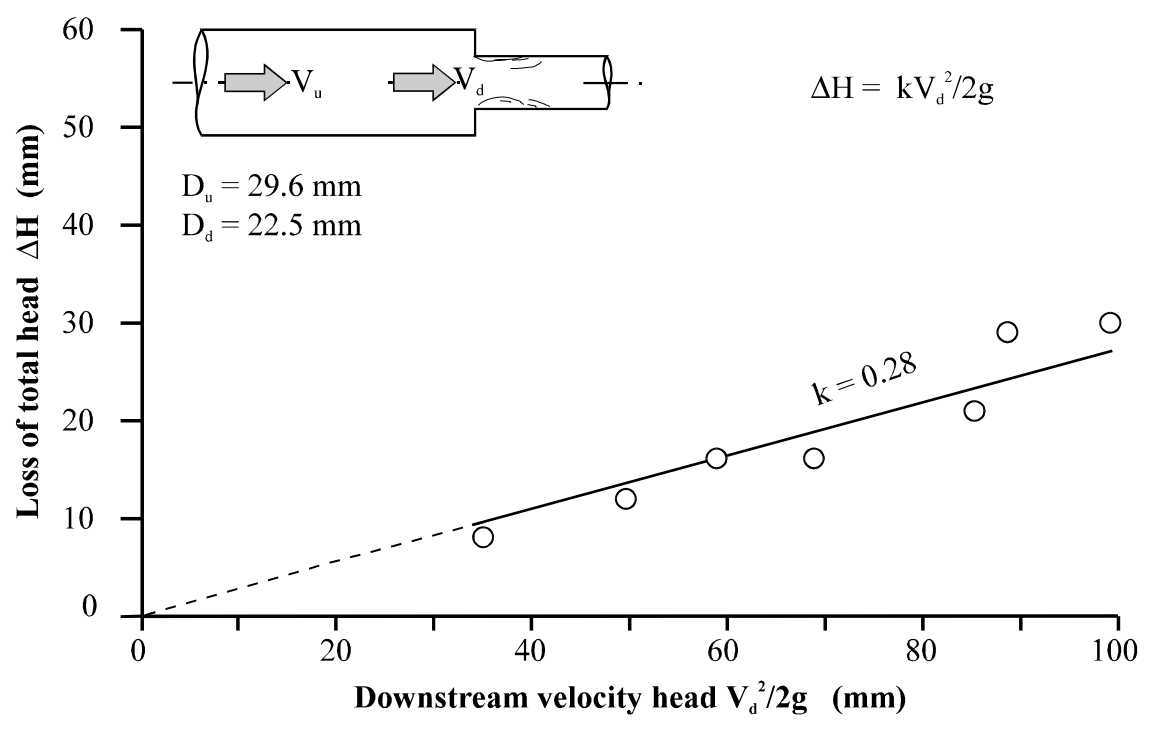


Figure 10.5 Total head loss ΔH in 90° bends of various radii



(a) Loss at sudden enlargement



(b) Loss at sudden contraction

Figure 10.6 Total head loss ΔH at a sudden enlargement and at a sudden contraction
 Figs 10.5 and 10.6 show the total head losses ΔH plotted against velocity head for each of the fittings. In the cases of the mitre, elbow and bend, the tube diameter is

22.5 mm, so the appropriate velocity head is obviously $V_1^2/2g$. For the enlargement and for the contraction, the relevant value is the velocity head in the pipe of smaller diameter, which again is $V_1^2/2g$. In each case, the results lie reasonably well on a straight line through the origin. The slope of the line gives the value of K for the fitting. The results are collected in Table 10.4.

Fitting		K
90° mitre	R/D = 0.50	1.34
90° elbow	R/D = 1.56	0.86
90° bend	R/D = 3.07	0.32
Enlargement	$D_u/D_d = 0.76$	0.25
Contraction	$D_u/D_d = 1.32$	0.28

Table 10.4 Experimental values of loss coefficient K

Discussion of Results

The results for the mitre, elbow and bend show that the loss coefficient K falls substantially as the radius of the bend is increased. Many previous experiments have indicated that, with a value of Re around 2×10^4 , K would be expected to reduce, from a value of about 1.4 for the mitre bend, to a value around 0.3 when $R/D = 3$. The values obtained in this experiment are in good agreement with these expectations.

For the enlargement, Equation (10.6) provides a theoretical value of K . In this case, this theoretical value is

$$K = \left[1 - \frac{A_u}{A_d} \right]^2 = \left[1 - \frac{3.98}{6.88} \right]^2 = 0.18$$

The measured value is significantly higher, at 0.25. Perhaps the piezometer tapping downstream of the enlargement is placed too close to allow the full recovery of piezometric pressure to take place. Moreover, the value of Δh_f is in this case about one half that of ΔH . Therefore, if there is significant error in the computed effect of pipe friction, there will be a noticeable effect on the resulting value of K . For the contraction, there is no theoretical value of K . However, Equation (10.8) may be used to calculate V_c/V_d from the measurements:

$$\text{viz } \left[\frac{V_c}{V_d} - 1 \right]^2 = 0.28 \text{ from which } \frac{A_c}{A_d} = \frac{V_d}{V_c} = 0.65$$

This is a plausible value for the contraction coefficient of the jet at entry the contracted pipe, and it lies between the extreme values of about 0.6 and 1.0 discussed earlier.

Questions for Further Discussion

1. What suggestions do you have for improving the apparatus?
2. No correction has been made to the differential piezometer readings for the difference in heights between the piezometer tapings. Can you explain why it would be wrong to make any such correction?
3. What are the sources of error? In particular, what percentage error in the value of K for any of the bends would result from an error of 0.1 mm in the measured diameter D_1 ? (1.8% approximately).
4. The effect of wall friction over the length of pipe between the piezometers has been estimated, from standard pipe friction data, at a single flow rate. Would a better result be obtained by estimating the friction effect over the range of flow rates?